Frascati Physics Series Vol. 69 (2019)
PHOTON 2019 - International Conference on the Structure and the Interactions of the Photon
Jun 3-7, 2019

VERY-FORWARD PHOTON PRODUCTION IN p-p AND p-Pb COLLISIONS MEASURED BY THE LHCf EXPERIMENT

Alessio Tiberio
Università degli Studi di Firenze and INFN, Sesto Fiorentino, Italy
on behalf of the LHCf Collaboration

Abstract

The main purpose of the LHCf experiment is to test the hadronic interaction models used in ground based cosmic rays experiments to simulate air-showers induced by ultra-high-energy cosmic rays in the Earth atmosphere. The LHCf experiment, situated at the LHC accelerator, is composed of two independent detectors located at 140 metres from the ATLAS interaction point (IP1) on opposite sides along the beam axis: the particular position of the detectors allows LHCf to measure neutral particles up to zero-degree with respect to the beam, with a pseudorapidity coverage of $\eta > 8.4$. Each detector is composed by two sampling and position sensitive calorimeters.

In this contribution the latest photon production measurements from LHCf will be compared with the predictions of DPMJET, EPOS, PYTHIA, QGSJET and SIBYLL Monte Carlo event generators, commonly used in air-shower simulations. The photon production cross section in proton-proton collisions at $\sqrt{s} = 13$ TeV and in proton-lead collisions at $\sqrt{s_{NN}} = 8.16$ TeV will be presented, including the preliminary combined analysis with ATLAS. There is not any hadronic interaction model well reproducing all the experimental data measured by the LHCf experiment. However, these data in the very-forward region will be useful in the tuning of the models and consequently reducing the discrepancy between their predictions.

1 Introduction

The LHC-forward experiment (LHCf) has measured neutral particles production in a very forward region in proton-proton and proton-lead collisions at the Large Hadron Collider. The main purpose of LHCf is to improve hadronic interaction models of Monte Carlo (MC) simulations used in cosmic rays indirect measurements. Highest energy cosmic rays can only be detected from secondary particles which are produced in the interaction of the primary particle with nuclei of the atmosphere, the so-called air showers.

Studying the development of air showers, it is possible to reconstruct the type and kinematic parameters of primary particles. To reproduce the development of air showers, MC simulations with accurate hadronic interaction models are needed. Since the energy flow of secondary particles is concentrated in the forward direction, measurements of particle production in the high pseudorapidity region (i.e. small angles) are very important. In the very forward region soft QCD interactions dominates and MC simulations of air showers utilize phenomenological models base on Gribov-Regge theory [1, 2]. Therefore, inputs from experimental data are crucial for the tuning of that models. The LHC accelerator gives the possibility to study a wide range of collision energies, from 0.9 TeV to 13 TeV in the center of mass frame, which corresponds to an energy range in the laboratory frame from 10^{14} eV to 0.9×10^{17} eV. This energy range covers the "knee" region of cosmic rays spectrum, which occurs around 10^{15} eV. Data collected by central detectors with 7 TeV collisions were already used for the tuning of hadronic interaction models widely used in air shower simulations (EPOS-LHC [3], QGSJET II-04 [4] and SIBYLL 2.3 [5]). However, discrepancies between observed data and MC simulations were observed also with these models [6].

2 The Detector

LHCf is composed of two independent detectors, called *Arm1* and *Arm2*. Arm1 is located 140 meters away from ATLAS interaction point (IP1) in the IP8 direction, while Arm2 is placed 140 meters away from IP1 in the opposite direction (toward IP2). Detectors are placed inside Target Neutral Absorber (TAN), where the beam pipe turns into two separates tubes. Since charged particles are deviated by the D1 dipole magnet (which bends colliding beams into the two separate beam pipes), only neutral particles, mainly photons and neutrons, reach the detector.

Each detector is made of two sampling and imaging calorimeters (called *towers* hereafter). Each tower is composed of 16 tungsten layers and 16 scintillator layers to measure the energy deposit and it also contains 4 position sensitive layers. During 0.9 TeV, 2.76 TeV and 7 TeV operations at the LHC, plastic scintillators (EJ-260) were used. Arm1 detector used scintillating fiber (SciFi) to measure position, while Arm2 used silicon microstrip detectors. For 13 TeV operation both detectors were upgraded: all the plastic scintillators were replaced by Gd_2SiO_5 (GSO) scintillators because of their radiation hardness; also the Arm1 SciFi were replaced by GSO bars. In Arm2 the signal of silicon detectors was reduced using a new bonding scheme of the microstrips to avoid saturation of readout electronics due to the higher energy deposit expected at $\sqrt{s} = 13$ TeV.

Transverse cross sections of towers are 20×20 mm^2 and 40×40 mm^2 for Arm1 and 25×25 mm^2 and 32×32 mm^2 for Arm2. Longitudinal dimension of towers is of 44 radiation lengths, which correspond to 1.6 nuclear interaction lengths. Energy resolution is better than 2% for photons above 200 GeV and of about 40% for neutrons. Position resolution for photons is 200 μm and 40 μm for Arm1 and Arm2, respectively, while position resolution for neutrons is of about 1 mm. Smaller tower of each detector is placed on the beam center and covers the pseudo-rapidity range $\eta > 9.6$, while larger tower covers the pseudo-rapidity range $8.4 < \eta < 9.4$. More detailed descriptions of detector performance are reported elsewhere [7, 8, 9, 10].

3 Physics Results With Proton-Proton Collisions At $\sqrt{s} = 13$ TeV

Results for inclusive photon energy spectrum in p-p collisions at $\sqrt{s} = 900$ GeV and 7 TeV have already been published [11, 12]. Proton-proton collisions at $\sqrt{s} = 13$ TeV were produced for the first time in 2015 at LHC. LHCf had a dedicated low-luminosity run from 9th to 13th of June 2015, with an instantaneous

luminosity of $0.3 \div 1.6 \times 10^{29}\mathrm{cm}^{-2}\mathrm{s}^{-1}$. The data sample used in this analysis was obtained during the LHC Fill #3855 in a 3-hours run started at 22:32 on July 12. The instantaneous luminosity measured by ATLAS [13] ranged from 3 to 5 $\times 10^{28}\mathrm{cm}^{-2}\mathrm{s}^{-1}$ during this subset of the run. The beams had 29 colliding bunches, an half crossing angle of 145 μrad, a β^* of 19 m, and a pile-up parameter of $\sim$0.01. The integrated luminosity recorded was 0.191 nb^{-1} for both Arm1 and Arm2.

3.1 Photon inclusive energy spectrum

The inclusive energy spectrum of photon produced in p-p collisions at $\sqrt{s} = 13$ TeV [14] is presented in fig.1 for two pseudo-rapidity ranges together with the predictions of DPMJET 3.06 [15, 16], EPOS-LHC, PYTHIA 8.212 [17, 18], QGSJET II-04 and SIBYLL 2.3 hadronic interaction models. The LHCf data lie between MC predictions but there is not an unique model with a good agreement in the whole energy range and in both rapidity regions. In the pseudorapidity range $\eta > 10.94$, QGSJET and EPOS presents a good overall agreement with experimental data; SIBYLL predicts a lower yield of photons, even if it features a shape similar to data; PYTHIA spectrum agrees with data until $\sim$3.5 TeV but become harder at higher energies; DPMJET is generally harder than data. In the pseudorapidity range $8.81 < \eta < 8.99$, EPOS and PYTHIA spectra agree with data until $\sim$3 TeV, while they become harder at higher energies; SIBYLL has a good agreement until $\sim$ 2 TeV, then also it becomes harder than data; QGSJET presents a lower yield of photons, while DPMJET generally predict an harder spectrum than experimental data.

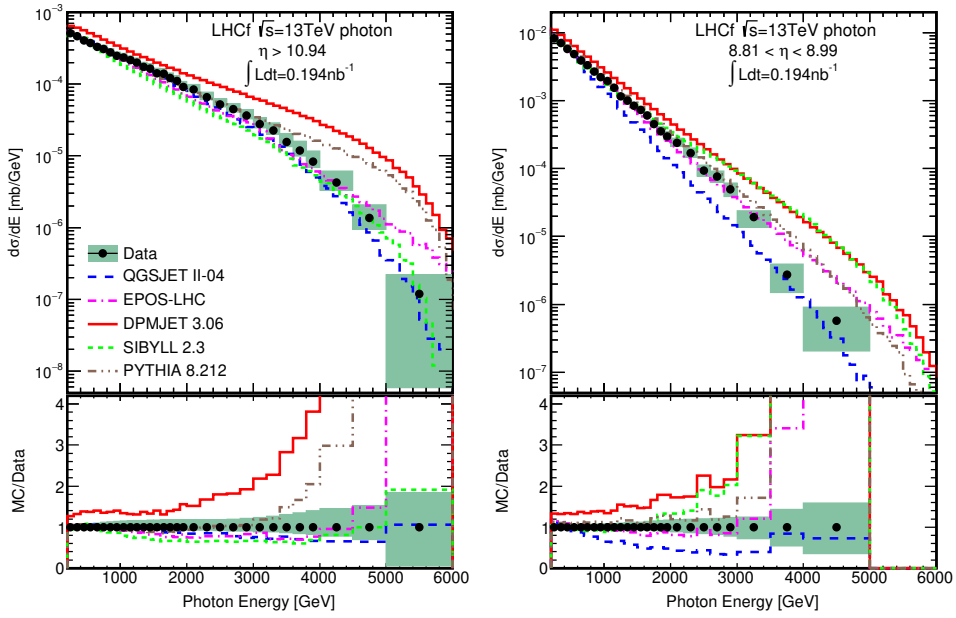

Figure 1: *Photon differential production cross section in the pseudorapidity regions $\eta > 10.94$ (left) and $8.81 < \eta < 8.99$ (right) for p-p collisions at $\sqrt{s} = 13$ TeV. Data are represented by black points while MC prediction from several models are represented by coloured histograms. Green shaded area represents statistical+systematic errors of data. Bottom panels show the ratio of MC predictions to data.*

3.2 LHCf-ATLAS combined analysis

The LHCf experiment alone does not have any information about the type of collision occured at the interaction point. Since 2013 LHCf and ATLAS [19] experiments exchange the trigger signals during LHCf dedicated runs, so it is possible to perform a combined analysis with the event information from both experiments. The number of tracks recorded by ATLAS detectors in the central region can be used to discriminate diffractive events from non-diffractive ones [20]. In particular, selecting events with no charged particles in the region $-2.5 < \eta < 2.5$ a pure sample of low-mass ($M_X < 20$ GeV) diffraction events can be selected.

The preliminary results [21] of the combined analysis are presented in fig.2, where the photon energy spectrum is shown for both the inclusive and the low-mass diffraction component. The diffraction spectrum of EPOS model has a good agreement with data in the $\eta > 10.94$ region, while PYTHIA has a better agreement for $8.81 < \eta < 8.99$.

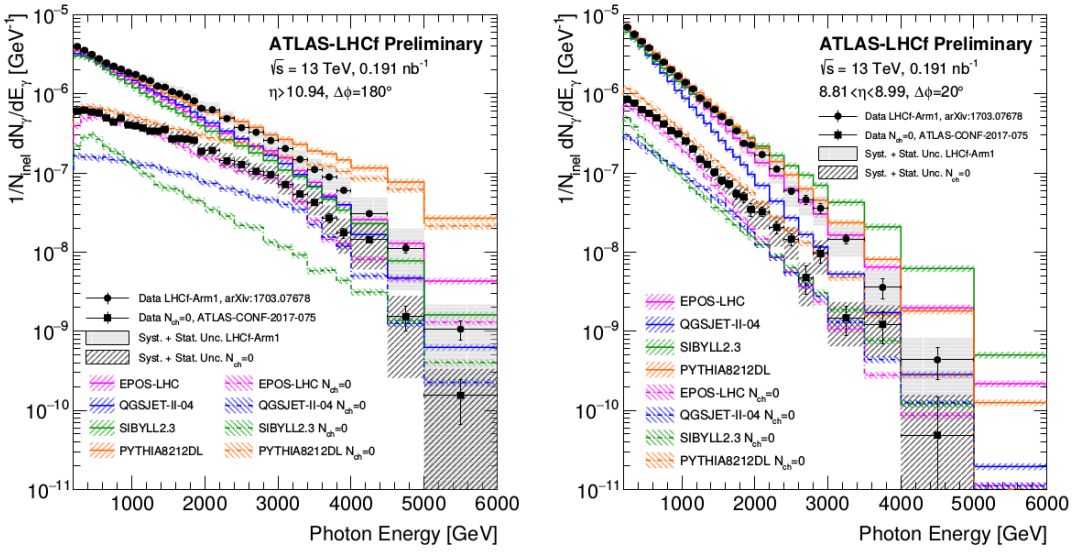

Figure 2: *Photon energy spectrum for pseudorapidity region* $\eta > 10.94$ *(left) and* $8.81 < \eta < 8.99$ *(right). Data are represented by black circles (inclusive) or black squares (low-mass diffraction), while MC predictions are represented by coloured solid (inclusive) or dashed (low-mass diffraction) lines. Hatched areas show statistical+systematic errors for data and statistical errors for MC. All the spectra are normalized to the total number of inelastic collisions.*

4 Physics Results With Proton-Lead Collisions At $\sqrt{s_{NN}} = 8.16$ TeV

A 9-hours-long low luminosity dedicated run for LHCf was performed on the 25th of November 2016 with proton-lead collisions at $\sqrt{s_{NN}} = 8.16$ TeV. Arm2 detector was installed on the proton-remnant side, while Arm1 detector was replaced by ATLAS ZDC. The data sample used to perform the photon production cross section analysis corresponds to an integrated luminosity of 8.1 μb^{-1} ($\sim$ 2 hours of operation). The instantaneous luminosity was $\sim 0.8 \times 10^{28} cm^{-2} s^{-1}$ with a pile-up parameter of 0.01.

The preliminary result of inclusive photon differential production cross section in p-Pb collisions at $\sqrt{s_{NN}} = 8.16$ TeV is presented in fig.3 for two pseudo-rapidity ranges together with the predictions

of DPMJET 3.06, EPOS-LHC and QGSJET II-04 hadronic interaction models. Unlike the p-p case, in p-Pb collisions also Ultra Peripheral Collisions (UPC) can occur when the colliding proton interacts with a virtual photon of the strong electromagnetic field of the lead nucleus. UPC are simulated combining STARLIGHT [22] to estimate the virtual photon flux, SOPHIA [23] for low-energy proton-photon collisions, and either DPMJET 3.05 ora PYTHIA 6.428 for high-energy proton-photon collisions. UPC contribution in then added to hadronic interaction models predicitons.

In the $\eta > 10.94$ psedurapidity region EPOS and QGSJET show a good agreement with data while DPMJET predicts an harder spectrum. For $8.81 < \eta < 8.99$ EPOS has a good agreement with data up to 2 TeV, while QGSJET predicts a lower yield and DPMJET an harder spectrum.

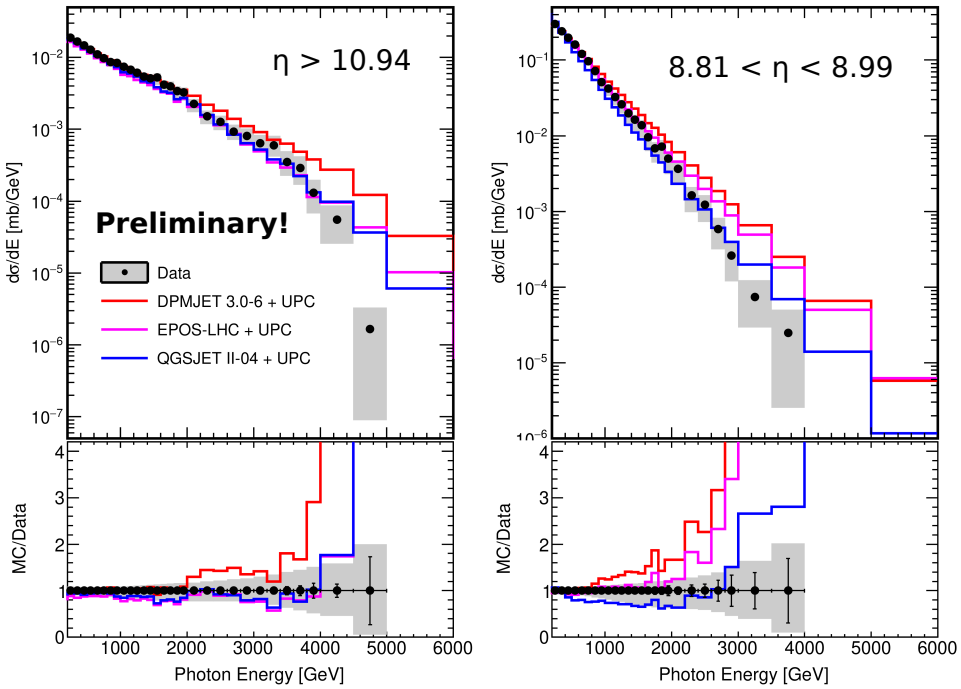

Figure 3: *Preliminary photon differential production cross section in the pseudorapidity regions* $\eta > 10.94$ *(left) and* $8.81 < \eta < 8.99$ *(right) for p-Pb collisions at* $\sqrt{s_{NN}} = 8.16$ *TeV. Data are represented by black points while MC prediction from several models are represented by coloured histograms. Grey shaded area represents statistical+systematic errors of data. Bottom panels show the ratio of MC predictions to data.*

5 Summary

LHCf experiment performed measurements on very forward photon production in proton-proton collisions at $\sqrt{s} = 13$ TeV and proton-lead collisions at $\sqrt{s_{NN}} = 8.16$ TeV at the LHC accelerator. These measurements are necessary to calibrate hadronic interaction models used in cosmic rays physics to understand the development of atmospheric showers. Measured photon inclusive production cross section in both p-p and p-Pb collisions indicates that there is not an unique model representing the data in the pseudorapidity regions $\eta > 10.94$ and $8.81 < \eta < 8.99$. However, the measured data lie between the prediction of DPMJET, EPOS, PYTHIA, QGSJET and SIBYLL hadronic interaction models. EPOS-LHC model

has an overall better agreement with data than other models; QGSJET II-04 has a good agreement in the $\eta > 10.94$ region; PYTHIA 8.212 is consistent with data in the low energy region (below $\sim$3 TeV); SIBYLL 2.3 shows a good agreement below $\sim$2 TeV in the $8.81 < \eta < 8.99$ region; DPMJET 3.06 predicts an harder spectrum than data in both the rapidity regions. In the low-mass diffractition event sample selected with the LHCf-ATLAS combined analysis, EPOS has a good agreement in the $\eta > 10.94$ region, while PYTHIA is more accurate for $8.81 < \eta < 8.99$.

References

1. V. Gribov, Sov. Phys. J. Exp. Theor. Phys. **26**, 414 (1968).
2. T. Regge, Nuovo Cimento **14**, 951 (1959).
3. K. Werner, F.-M. Liu, and T. Pierog, Phys. Rev. C **74**, 044902 (2006).
4. S. Ostapchenko, Nucl. Phys. B, Proc. Suppl. **151**, 143 (2006).
5. F. Riehn, Felix *et al.*, PoS ICRC2015 (2016) 558.
6. The Pierre Auger Collaboration, PRL **117** (2016) 192001.
7. O. Adriani *et al.*, JINST **3**, S08006 (2008).
8. O. Adriani *et al.*, JINST **5**, P01012 (2010).
9. Y. Makino, A. Tiberio *et al.*, 2017 JINST **12** P03023.
10. K. Kawade *et al.*, JINST **9**, P03016 (2014).
11. O. Adriani *et al.*, Physics Letters B **703**, 128-134 (2011).
12. O. Adriani *et al.*, Physics Letters B **715**, 298-303 (2012).
13. ATLAS collaboration, Eur. Phys. J. C **76** (2016) 653.
14. O. Adriani *et al.*, Physics Letters B **780** (2018) 233–239
15. F. W. Bopp, J. Ranft, R. Engel, and S. Roesler, Phys. Rev. C **77**, 014904 (2008).
16. R. Engel, J. Ranft, and S. Roesler, Phys. Rev. D **55**, 6957 (1997).
17. T. Sjöstand, S. Mrenna, and P. Skands, J. High Energy Phys. **05** (2006) 026.
18. T. Sjöstand, S. Mrenna, and P. Skands, Comput. Phys. Commun. **178**, 852 (2008).
19. ATLAS Collaboration, The ATLAS Experiment at the CERN Large Hadron Collider, JINST **3** (2008) S08003.
20. Q. D. Zhou *et al.*, Eur. Phys. J. C **77** (2017) no.4, 212
21. The ATLAS and LHCf Collaborations, ATLAS-CONF-2017-075
22. http://starlight.hepforge.org
23. A. Mücke, R. Engel, J. P. Rachen, R. J. Protheroe, and T. Stanev, Comput. Phys. Commun. **124**, 290 (2000).